# Quantum Monte Carlo Studies of Density Functional Theory

Maziar Nekovee,[1] W. Matthew C. Foulkes,[2] and Richard J. Needs[3]

[1] *Complexity Research Group, Antares Building PP5, BTexact Technologies Martlesham, Suffolk IP5 3RE, UK,*
[2] *The Blackett Laboratory, Imperial College, Prince Consort Road, London SW7 2BZ, UK*
[3] *Cavendish Laboratory, Madingley Road, Cambridge CB3 0HE, UK*

**Abstract**

We review our variational quantum Monte Carlo approach for evaluating the key quantities in the density functional theory of inhomogeneous many-electron systems, and describe the underlying simulation algorithm and its parallel implementation. We discuss the insights gained from our recent application of the method to the study of the density functional theory of the strongly inhomogeneous electron gas.

*Key words:* Quantum Monte Carlo, Density Functional, Exchange-Correlation
*PACS:* 71.15.Mb, 71.10.-w, 71.45.Gm

## 1 Introduction

An essential prerequisite for accurate first-principles simulations of the electronic properties of materials is an adequate description of the many-body effects caused by the long-ranged Coulomb interactions acting between $\sim 10^{23}$ electrons which comprise a macroscopic piece of material. The standard computational tool for the treatment of these effects in many-electron systems is density functional theory (DFT) [1], the inventor of which, Walter Kohn, received the 1998 Nobel prize in Chemistry. The application of DFT relies heavily on finding accurate approximations for the exchange-correlation energy functional, $E_{\rm xc}[n(\mathbf{r})]$, which describes many-body effects in terms of the electron density $n(\mathbf{r})$. The most frequently used approximations to date are the local density approximation (LDA) and the generalized gradient approximation (GGA) [2–4]. Given its simplicity (see section (4)), the LDA works surprisingly well, but not well enough for many important applications of DFT to surface chemistry, quantum chemistry and biology. Although often better

than the LDA, GGA functionals are unable to consistently deliver the very high chemical accuracy which is often required in such applications. The quest for improved approximations to $E_{xc}$ is the subject of much current research.

Quantum Monte Carlo (QMC) simulations [5] provide the state-of-the-art alternative approach to the many-body problem in real materials [6]. These methods are based on sampling the full many-body wavefunction of the system, and are capable of describing many-body effects in inhomogeneous systems with an accuracy which is typically an order of magnitude better than LDA-based DFT [6,7]. The aim of the research presented in this paper has been the development of QMC as a tool for investigating density functional theory in inhomogeneous many-electron systems, in order to open a new direction in the search for improved functionals.

Exchange-correlation effects arise from the electrostatic interaction between an electron and the exchange-correlation hole $n_{\rm xc}$ that surrounds it [8]. The exchange-correlation hole is the key quantity used in analyzing the LDA and the starting point for almost all attempts to go beyond it. We have developed a variational quantum Monte Carlo (VMC) method for calculating $n_{\rm xc}$ and the corresponding exchange-correlation energy density $e_{\rm xc}$ of inhomogeneous systems [9], and have implemented our algorithm on massively parallel platforms. In this paper, we outline our method and discuss its parallel implementation, which has enabled us to study systems with a large number of electrons. We describe a very recent application of the method to the study of DFT in strongly inhomogeneous electron gases [10], and the insight gained from the comparison of our results for these systems with those obtained from the LDA and the GGA.

## 2 Methodology

### *2.1 Coupling Constant Formula*

Using a coupling-constant integration technique [8], the exchange-correlation energy can be written as (throughout this paper we use Hartree atomic units in which $e = m = 4\pi\epsilon_0 = \hbar = 1$)

$$E_{xc}[n(\mathbf{r})] = \frac{1}{2}\int d\mathbf{r}\int d\mathbf{r}'\,\frac{n(\mathbf{r})n_{xc}(\mathbf{r},\mathbf{r}',[n])}{|\mathbf{r}-\mathbf{r}'|} = \int d\mathbf{r}\; e_{xc}(\mathbf{r},[n])\;. \qquad (1)$$

Note that both $n_{xc}$ and $e_{xc}$ are (unique) functionals of the electron density, i.e. the value of $e_{xc}$ evaluated at a point $\mathbf{r}$ depends on the value of electron density of the system everywhere. We have indicated this functional dependence using

square brackets. The exchange-correlation hole is obtained from the following coupling- constant integral [8]:

$$n(\mathbf{r})n(\mathbf{r}') + n(\mathbf{r})n_{xc}(\mathbf{r},\mathbf{r}',[n]) = \int_0^1 d\lambda \, \langle \Psi^\lambda | \sum_i \sum_{j(\neq i)} \delta(\mathbf{r}-\mathbf{r}_i)\delta(\mathbf{r}'-\mathbf{r}_j) | \Psi^\lambda \rangle \; . \quad (2)$$

In the above equation, $\Psi^\lambda$ is the antisymmetric ground state of the Hamiltonian $H^\lambda$ associated with coupling $\lambda$:

$$\hat{H}^\lambda = \hat{T} + \lambda \hat{V}_{ee} + \hat{V}^\lambda \; . \quad (3)$$

Here $\hat{T}$ and $\hat{V}_{ee}$ are the operators for the kinetic and electron-electron interaction energies, and $\hat{V}^\lambda = \Sigma V^\lambda(\mathbf{r}_i)$ is the as yet unknown potential needed to hold the electron density $n^\lambda(\mathbf{r})$ associated with $\Psi^\lambda$ equal to $n(\mathbf{r})$ for all values of $\lambda$ between 0 and 1. [1]

### *2.2 Constrained Variance Maximization*

Given an interacting many-body system with ground-state density $n(\mathbf{r})$, the main ingredient for evaluating $n_{xc}$ and $e_{xc}$ is the many-body wavefunction $\Psi^\lambda$ for systems corresponding to different values of the coupling constant $\lambda$. In conventional variational Monte Carlo calculations, an overall fit to $\Psi^\lambda$ is obtained using a variance-reduction technique [5,12,13]. In this method one determines the parameters $\{\alpha\}$ in the trial function $\Psi_T^\lambda(\mathbf{R},\{\alpha\})$ by minimizing the variance $\sigma^2$ of the local energy:

$$\sigma^2 = \int d\mathbf{R} \; \left[ \frac{H^\lambda \Psi_T^\lambda(\mathbf{R})}{\Psi_T^\lambda(\mathbf{R})} - E[\Psi_T^\lambda] \right]^2 |\Psi_T^\lambda(\mathbf{R})|^2 . \quad (4)$$

Here $E[\Psi_T^\lambda]$ is the expectation value of $H^\lambda$, and $\sigma^2$ reaches its lower bound (of zero) if and only if $\Psi^\lambda$ is an exact eigenfunction of this Hamiltonian.

The above unconstrained optimization cannot be directly applied in the case of coupling constant integration since the Hamiltonian contains the unknown potential $V^\lambda$. Our approach [9] to this problem is a generalization of the scheme used by Hood *et al* [11]. It amounts to treating *both* $\Psi^\lambda$ and $V^\lambda$ variationally and determining the variational parameters by simultaneously minimizing the variance of the local energy and the deviations of $n^\lambda$ from $n$. This is achieved by

[1] The potential $V^\lambda(\mathbf{r})$ at point $\mathbf{r}$ is the Lagrange multiplier corresponding to the fixed-density constraint at that point.

expanding $n(\mathbf{r})$ and $n^{\lambda}(\mathbf{r})$ in a complete and orthonormal set of basis functions (with a suitably chosen cutoff $N_d$) and defining a modified penalty function $\mu^2$

$$\mu^2 = \sigma^2 + W \sum_{s=1}^{N_d} \left[ n_s - n_s^{\lambda} \right]^2 , \tag{5}$$

where $W$ is a weight factor, the magnitude of which determines the emphasis laid on the fixed-density constraint [2], and $n_s$ and $n_s^{\lambda}$ are the expansion coefficients of the target density $n(\mathbf{r})$ and the density produced from the trial wavefunction $\Psi_T^{\lambda}$, respectively. The above penalty function reaches its lower bound (of zero) if and only if $\Psi^{\lambda}$ is the exact many-body wavefunction satisfying the fixed-density constraint (within the accuracy set by $N_d$) and $V^{\lambda}$ is the corresponding exact potential. Hence, maximization of $\mu^2$ will, in principle, result in the *simultaneous* determination of $\Psi^{\lambda}$ and $V^{\lambda}$. In practice, of course, our constrained search is restricted to a sub-space of many-body wavefunctions, and maximization of $\mu^2$ yields an optimal fit to $\Psi^{\lambda}$ and a corresponding optimal fit to $V^{\lambda}$.

### *2.3 Numerical algorithm and parallel implementation*

Our numerical implementation of the above scheme works as follows. We start with initial guesses for the many-body wavefunction $\Psi^{\lambda}$ and the one-body potential $V^{\lambda}$. A fixed number $N_c$ of statistically-independent configurations $\mathbf{R}_i$ are then sampled from $|\Psi^{\lambda}|^2$ using the Metropolis algorithm. Next, the Monte Carlo estimator of $\sigma^2$ and the expansion coefficients of the electron density, $n_s^{\lambda}$, are evaluated, from which the value of the penalty function $\mu^2$ is obtained. The variational parameters in $\Psi^{\lambda}$ and $V^{\lambda}$ are then varied, using a standard NAG optimization routine, until $\mu^2$ is minimized. For each value of $\lambda$, this procedure is repeated several times until the variational coefficients reach convergence. Once the optimal $\Psi^{\lambda}$s are obtained, we evaluate $n_{xc}^{\lambda}$ and $e_{xc}^{\lambda}$ to a desired accuracy from a set of long VMC runs. Finally, $e_{xc}$ and $n_{xc}$ are obtained by performing the coupling-constant integration using ordinary numerical integration methods. In the calculations reported here 6 values of $\lambda$ were used.

The parallelization of the VMC code was performed using the task-farming model, wherein all processors execute precisely the same program on different

[2] We found that setting $W$ equal to the number of configurations results in a satisfactory minimization of both the variance in energy and the error in electron density.

data. Given a variational wavefunction $\Psi^\lambda$, each processor undergoes a separate "random walk" in the configuration space of all electrons and generates, after an equilibration period, an independent set of statistically uncorrelated points sampled from $|\Psi^\lambda|^2$. Interprocessor communication is needed only for the final collation of results. The parallelization of the optimization code is more complex and, following [13], is performed using the master-slave programming model in which one processor, the master, delegates works to the other processors, the slaves, who complete their own share of the work and return it to master for final processing. The numerical optimization routine runs on the master processor and broadcasts the initial values of the variational parameters to the slaves. Each of the slaves stores a subset of electron configurations in memory and, upon receiving values of the variational parameters, evaluates the contributions to the variance $\sigma^2$ of the local energy and the expansion coefficients $n_s$ of the electron density for its subset of configurations. These are returned to the master, which evaluates the penalty function $\mu^2$, and, via a NAG minimization routine, determines new values of the variational parameters. Communication between processors and synchronization are performed using the message passing standard MPI. The parallel codes were implemented on the CRAY T3E massively-parallel computer at Edinburgh Parallel Computing Centre, which is a distributed- memory platform with a multiple-instruction multiple-data (MIMD) architecture.

## 3 Exchange and Correlation in the Strongly Inhomogeneous Electron Gas

We performed VMC coupling-constant simulations for finite spin-unpolarized electron gases contained in a face-centered cubic simulation cell subject to periodic boundary conditions. The average electron density was $n^0 = 3/(4\pi r_s^3)$, where $r_s$=$2a_0$ (approximately the same as for Al). The exact interacting ground-state density $n(\mathbf{r})$ was chosen *a priori*, and the constrained minimization scheme was then used to find, at each $\lambda$, the exact (within VMC) wave function $\Psi^\lambda$ and external potential $V^\lambda$ corresponding to that density. The input density $n(\mathbf{r})$ was generated using the procedure described in [10] and with an external potential of the form $V_q \cos(\mathbf{q}.\mathbf{r})$, where $V_q$ was fixed at $2.08\epsilon_F^0$ and $\epsilon_F^0$ is the Fermi energy corresponding to $n^0$. We considered three systems, corresponding to $q = 1.11k_F^0$, $1.55k_F^0$, and $2.17k_F^0$, and cells containing 64, 78, and 69 electrons, respectively. The simulations were performed using the following Slater-Jastrow ansatz as our many-body wave function:

$$\Psi^\lambda = D^\uparrow D^\downarrow \exp\left[-\sum_{i>j} u^\lambda_{\sigma_i,\sigma_j}(r_{ij}) + \sum_i \chi^\lambda(\mathbf{r}_i)\right] \tag{6}$$

where $r_{ij} = |\mathbf{r}_i - \mathbf{r}_j|$, $D^{\uparrow}$ and $D^{\downarrow}$ are Slater determinants of spin-up and spin-down Kohn-Sham orbitals [3], respectively, $u^{\lambda}_{\sigma_i,\sigma_j}$ is a two-body term correlating the motion of pairs of electrons ($\sigma_i$ denotes the spin of electron $i$) and $\chi^{\lambda}$ is a one-body term, which is crucial for a satisfactory description of strongly inhomogeneous systems [17]. At each $\lambda$ we used a total of 20 variational parameters in $\Psi^{\lambda}$ and up to 7 coefficients in the Fourier series expansions of $n^{\lambda}$ and $V^{\lambda}$. After the optimization runs the expectation values were calculated using $10^6$ independent configurations of all the electrons. The statistical errors were found to be negligible except in $n_{xc}$ in low-density regions, where they were much smaller that the differences between $n_{xc}$ and $n^{LDA}_{xc}$. Finite-size effects were mitigated using the methodology described in [10].

### *3.1 Exchange-correlation holes*

To provide a detailed visualization of the behavior of the exchange-correlation holes, we used our VMC data to produce an animation of the deformation of the hole around an electron which moves in one of our systems (the $q = 1.11k^0_F$ system) along a line parallel to $\mathbf{q}$ (the direction of maximum inhomogeneity) from a density maximum toward the tail of $n(\mathbf{r})$. This system resembles a periodic array of thin metallic slabs with a vacuum gap between them, and the results are relevant to understanding exchange-correlation at metallic surfaces.

Fig. 1 shows snapshots of these animations. The XC hole is displayed as a function of $\mathbf{r}'$ around a fixed electron at $\mathbf{r}$, with $\mathbf{r}'$ ranging in a plane parallel to $\mathbf{q}$. Also shown is the corresponding LDA hole, $n^{LDA}_{xc}$, [8] and the electron density profile. At the density maximum (left panel), both $n^{VMC}_{xc}$ and $n^{LDA}_{xc}$ are centered at the electron. However, unlike $n^{LDA}_{xc}$, which is always spherically symmetric, $n^{VMC}_{xc}$ is contracted in the direction of the inhomogeneity. As the electron moves away from the density maximum to a point on the slope (middle panel), the nonlocal nature of $n^{VMC}_{xc}$ becomes manifest. While $n^{LDA}_{xc}$ is still centered at the electron and is rather diffuse, $n^{VMC}_{xc}$ lags behind near the density maximum and is much more compact. The nonlocal behavior of $n^{VMC}_{xc}$ becomes remarkable at the density minimum (right panel). Here $n^{VMC}_{xc}$ has two large nonlocal minima, each centered at a density maximum $\sim$2.80 a.u. away from the electron (the small fluctuations of $n^{VMC}_{xc}$ at this point are statistical errors). The LDA hole, by contrast, is spread over the whole system in order to satisfy the sum rule [8]: $\int d\mathbf{r}' n^{LDA}_{xc}(\mathbf{r}, \mathbf{r}') = -1$. This striking nonlocal behavior of $n^{VMC}_{xc}$ also occurs in the other two systems. The behavior of $n_{xc}$ at the density minima is analogous to the behavior of the exchange-correlation hole of an electron located just outside a metal surface [16].

[3] These orbitals are the lowest energy eigenfunctions of $H^{\lambda=0}$.

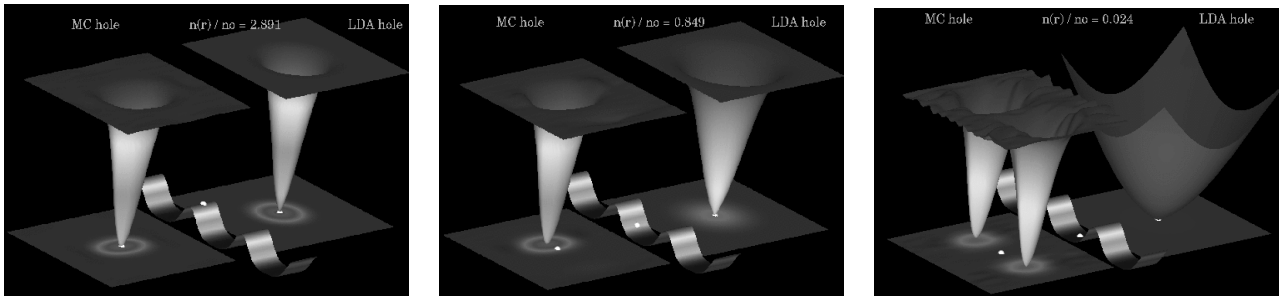


Fig. 1. The VMC and the LDA exchange-correlation holes, $n_{xc}(\mathbf{r}, \mathbf{r}')$, for a strongly inhomogeneous electron gas are shown (the $q = 1.11k_F^0$ system). The exchange-correlation hole is plotted for $\mathbf{r}$ at a density maximum (left), on the slope (middle), and at a density minimum (right), with $\mathbf{r}'$ ranging in a plane parallel to $\mathbf{q}$ (the direction of maximum inhomogeneity). The electron density is also shown schematically and the position of the electron is indicated by a white bullet.

### *3.2 Exchange-correlation energy densities*

In Fig. 2 we show $e_{xc}^{LDA} - e_{xc}^{VMC}$ and $e_{xc}^{GGA} - e_{xc}^{VMC}$ for two of the strongly inhomogeneous systems studied, where both $e_{xc}^{LDA}$ and $e_{xc}^{GGA}$ are calculated using the exact ground-state density $n(\mathbf{r})$ [4]. The results are plotted along a line parallel to $\mathbf{q}$ (we call this direction $y$). Also shown are $n(\mathbf{r})$ and $\nabla^2 n(\mathbf{r})$ plotted along the same line. It is apparent that the shape, magnitude, and sign of the LDA errors in $e_{xc}$ closely follow the shape, magnitude, and sign of $\nabla^2 n(\mathbf{r})$. The LDA errors in $e_{xc}$ are large and negative in regions where $\nabla^2 n(\mathbf{r})$ is large and negative (around density maxima), and large and positive in regions where $\nabla^2 n(\mathbf{r})$ is large and positive. The GGA performs much better than the LDA in the tail regions but does not improve the LDA near the density maxima. This is because the GGA corrections to the LDA are *by construction* always positive, and so have the wrong sign near a density maximum where the LDA overestimates $e_{xc}$ (in absolute value). Similar behavior has been observed also in the silicon atom [15] and in molecules[14]. In these systems, the negative LDA errors around the density maxima are overcompensated by positive errors in the bonding and outer regions and hence the GGA corrections result in a net improvement over the LDA of the integrated $E_{xc}$. In our systems, the LDA errors in $E_{xc}$ change sign from positive (for the $q$=$1.11k_F^0$ system) to negative (for the two other systems) as $q$ increases, and the negative contributions to $\Delta e_{xc}$, which occur where $\nabla^2 n(\mathbf{r}) < 0$, become dominant. Consequently, the GGA corrections improve $E_{xc}^{LDA}$ for the $q$=$1.11k_F$ system but worsen it for

[4] Strictly speaking, $e_{xc}^{GGA}$ does not directly correspond to the $e_{xc}$ obtained from $n_{xc}$ because of an integration by part in construction of $e_{xc}^{GGA}$ from the gradient expansion of $n_{xc}$ [2]. Nevertheless, it gives a pointwise description of the exchange-correlation and for this reason we found it interesting to compare it with our VMC results.

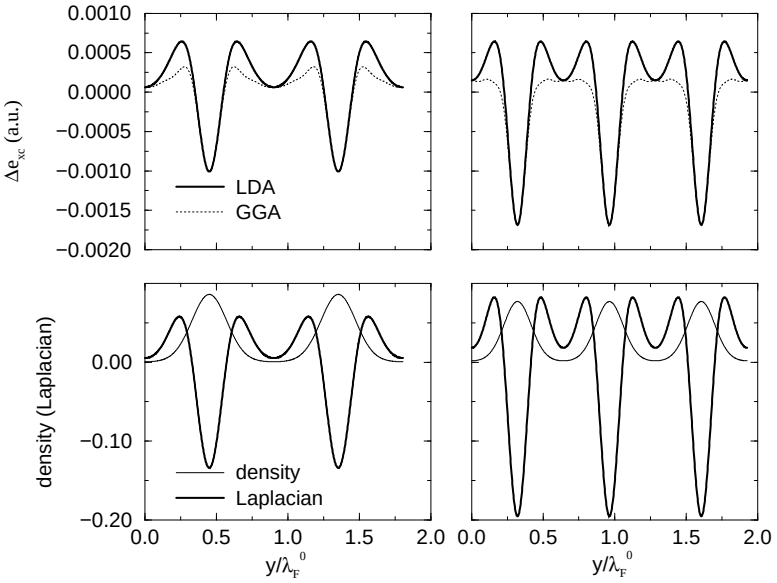


Fig. 2. The upper graph shows $e_{xc}^{LDA} - e_{xc}^{VMC}$ (heavy solid lines) and $e_{xc}^{GGA} - e_{xc}^{VMC}$ (light dotted lines) along a direction parallel to $\mathbf{q}$ for two different strongly inhomogeneous systems (corresponding to $q = 1.11k_F^0$ and $q = 1.55k_F^0$). The lower panel shows the corresponding electron densities (light lines) and Laplacians (heavy lines). Distances are given in units of the Fermi wavelenght $\lambda_F^0 = 2\pi k_F^0$.

the two other systems [10].

## 4 Towards Improved Semilocal Functionals

The exchange-correlation energy density is a unique functional of the electron density. Provided that the electron density has a convergent Taylor expansion about the point $\mathbf{r}$, one can therefore write

$$E_{xc}[n] = \int d\mathbf{r}\; e_{xc}(\mathbf{r},[n]) = \int d\mathbf{r}\; e_{xc}^{(\infty)}(\mathbf{r}, n(\mathbf{r}), \nabla_i n(\mathbf{r}), \nabla_i\nabla_j n(\mathbf{r}), \ldots) \qquad (7)$$

where $e_{xc}^{\infty}$ denotes a mapping from the density and all its gradients at $\mathbf{r}$ to $e_{xc}$. The LDA exchange-correlation energy is given by $E_{xc}^{LDA} = \int d\mathbf{r}\; e_{xc}^{hom}(n(\mathbf{r})) = \int d\mathbf{r} e_{xc}^{(1)}(n(\mathbf{r}))$, where $\mathrm{e}_{xc}^{hom}$ is the exchange-correlation energy density of a uniform electron gas with density $n = n(\mathbf{r})$. The LDA may be viewed as an approximation of $e_{xc}^{(\infty)}$ by a function of one variable, namely the electron density $n(\mathbf{r})$. In the GGA, an improved description is sought by incorporating the first gradient of the electron density $\nabla_i n(\mathbf{r})$:

$$E_{xc}^{GGA} = \int d\mathbf{r}\; e_{xc}^{GGA}(n(\mathbf{r}), |\nabla n(\mathbf{r})|) = \int d\mathbf{r} e_{xc}^{(2)}(n(\mathbf{r}), |\nabla n(\mathbf{r})|) \qquad (8)$$

where $e_{xc}^{GGA}$ is a suitably chosen non-linear function of two variables, the electron density and its first gradient. A natural extension is to employ the next variable, the Laplacian of the electron density $\nabla^2 n(\mathbf{r})$, in the approximation of $e_{xc}^{(\infty)}$, i.e.

$$e_{xc}^{(\infty)} \approx e_{xc}^{(3)}(n(\mathbf{r}), |\nabla n(\mathbf{r})|, \nabla^2 n(\mathbf{r})) \tag{9}$$

Approximations of this type has been recently put forward by several authors [19]. The results discussed in the previous section indicate that such approximations should be able to reach a significantly higher level of accuracy than current GGAs since $\nabla^2 n(\mathbf{r})$ provides a means to distinguish between the physically different regions around density maxima (where the LDA overestimates $e_{xc}$) and density minima (where the LDA underestimates $e_{xc}$), which is lacking in GGAs.

Such semilocal approximations can be viewed as an effort to find the (energetically) most accurate "projection" of $e_{xc}^{(\infty)}$ onto the finite space spanned by $n$, $|\nabla n|$ and $\nabla^2 n$. This task is significantly easier in the case of exchange energy $E_x$ since the scaling property [18]

$$E_x[\gamma^3 n(\gamma \mathbf{r})] = \gamma E_x[n(\mathbf{r})]; \qquad \gamma > 0 \tag{10}$$

implies that this quanity can be written as

$$E_x = \int d\mathbf{r}\; e_x(\mathbf{r}, [n]) = \int d\mathbf{r}\; e_x^{LDA}(n(\mathbf{r})) F_x(s, l, \ldots) \tag{11}$$

where $F_x$ is the so-called exchange enhancement factor and $s = |\nabla n|/(2k_F(\mathbf{r})n(\mathbf{r}))$, $l = \nabla^2 n/(4k_F^2(\mathbf{r})n(\mathbf{r}))$ are a dimensionless gradient and a dimensionless Laplacian, respectively. In atoms and some other systems, the electron density profile is such that there is a one-to-one mapping from $s$ to $l$: i.e. $l = l(s)$. The Laplacian variable can then be eliminated and a new single-variable enhancement factor, $\tilde{F}_x = \tilde{F}_x(s)$, defined, which may be parameterized using a GGA form. (This might explain why GGAs are so successful in atoms.) In our systems, however, the situation is almost reversed: i.e. $F_x$ was found to be an almost unique function of $l$ but could not be described uniquely in terms of the reduced gradient [10]. These results suggest that in order to find a "universal" form for $F_x(s, l)$ one should evaluate $F_x$ for many different systems, each representing a different class of electron densities. In this way, a complete "scatter map" of $F_x$ against $(s, l)$ can be obtained (within the physically relevant range of $s$ and $l$). This scatter map can then be used to find the energetically most accurate parameterization of $F_x$ in terms of $s$ and $l$. [5]

[5] There is of course no guarantee that the scatter mapping $(s, l) \to F_x$ will be one-to-one, since the exact $F_x$ is a function of all density gradients. One hopes, however,

## References


[1] P. Hohenberg and W. Kohn, Phys. Rev. **136**, B864 (1964); W. Kohn and L. J. Sham, Phys. Rev. **140**, A1133 (1965).

[2] J. P. Perdew, K. Burke, and M. Ernzerhof, Phys. Rev. Lett. **77**, 3865 (1996); J. P. Perdew and Y. Wang, Phys. Rev. B **33**, 8880 (1986).

[3] A. D. Becke, Phys. Rev. A **38**, 3098 (1988); A. D. Becke, J. Chem. Phys. **98**, 5648 (1993).

[4] C. Lee, W. Yang and R.G. Parr, Phys. Rev. B **37**, 785 (1988).

[5] B. L. Hammond, W. A. Lester, Jr., and P. J. Reynolds, *Monte Carlo Methods in Ab Initio Quantum Chemistry* (World Scientific, Singapore, 1994).

[6] For a recent review see W. M. C. Foulkes, L. Mitas, R. J. Needs and G. Rajagopal, Rev. Mod. Phys. **73**, 33 (2001).

[7] See, e.g., James B. Anderson's constribution to this volume.

[8] R. G. Parr and W. Yang, *Density Functional Theory of Atoms and Molecules* (Oxford University Press, Oxford, 1988).

[9] M. Nekovee, W. M. C. Foulkes, A. J. Williamson, G. Rajagopal and R. J. Needs, Adv. Quantum Chem. **33**, 189 (1999).

[10] M. Nekovee, W. M. C. Foulkes and R. J. Needs, Phys. Rev. Lett. **87**, 036401 (2001).

[11] R. Q. Hood, M. Y. Chou, A. J. Williamson, G. Rajagopal, R. J. Needs and W. M. C. Foulkes, Phys. Rev. Lett. **78**, 3350 (1997); Phys. Rev. B **57**, 8972 (1998).

[12] C. J. Umrigar, K. G. Wilson, and J. W. Wilkins, Phys. Rev. Lett. **60**, 1719 (1988).

[13] A. J. Williamson, S. D. Kenny, G. Rajagopal, A. James, R. J. Needs, L. M. Fraser, W. M. C. Foulkes and P. Maccalum. Phys. Rev. B **53**, 9640 (1996).

[14] P. R. T. Schipper, O. V. Gritsenko and E. J. Baerends, Phys. Rev. A **57**, 1729 (1998).

[15] A. Puzder, M. Y. Chou and R. Q. Hood, Phys. Rev. A **64**, 022501 (2001).

[16] M. Nekovee and J. M. Pitarke, Comp. Phys. Comm. **137**, 123 (2001).

[17] See S. Fahy, X. W. Wang, and S. G. Louie, Phys. Rev. Lett. **61**, 1631 (1998); R. Gaudoin, M. Nekovee, W. M. C. Foulkes, G. Rajagopal and R. J. Needs, Phys. Rev. B **63**, 115115 (2001).

[18] M. Levy and J. B. Perdew, Phys. Rev. A **32**, 2010 (1985).

[19] See, e.g., J. P. Perdew, S. Kurth, A. Zupan, and P. Blaha, Phys. Rev. Lett. **82**, 2544 (1999).


---

that the non-uniqueness of the mapping is energetically insignificant.